Analysis of acceptable spectral windows of quadratic cascaded nonlinear processes in a periodically poled lithium niobate waveguide

Kwang Jo Lee,[1,3,*] Sheng Liu,[1] Katia Gallo,[2] Periklis Petropoulos,[1] and David J. Richardson[1]

[1]*Optoelectronics Research Centre, University of Southampton, Southampton, SO17 1BJ, UK*
[2]*Department of Applied Physics, Royal Institute of Technology (KTH), 10691 Stockholm, Sweden*
[3]*Currently with Centre for Ultrahigh Bandwidth Devices for Optical Systems (CUDOS), School of Physics, University of Sydney, Sydney, New South Wales 2006, Australia*
** kjl@orc.soton.ac.uk*

Abstract: We report a systematic and comparative study of the acceptance bandwidths of two cascaded quadratic nonlinear processes in periodically poled lithium niobate waveguides, namely cascaded second-harmonic generation and difference-frequency generation (cSHG/DFG) and cascaded sum-frequency generation and difference-frequency generation (cSFG/DFG). We first theoretically and experimentally study the acceptance bandwidths of both the individual second-harmonic generation (SHG) and sum-frequency generation (SFG) processes in the continuous wave (CW) and pulsed-pump regimes. Our results show that the SHG bandwidth is approximately half that of the SFG process in the CW regime, whereas the SHG acceptance bandwidth can approach the CW SFG bandwidth limit when pulsed-pump is used. As a consequence we conclude that the tuning bandwidths of both cascaded processes should be similar in the pulsed pump regime once the pump pulse bandwidths approach that of SFG (i.e. the cSHG/DFG bandwidth is not limited by the CW SHG bandwidth). We confirm that this is the case experimentally.

OCIS codes: (060.4510) Optical communications; (130.3730) Lithium niobate; (190.2620) Harmonic generation and mixing; (190.4410) Nonlinear optics, parametric processes.

References and links

1. S. J. B. Yoo, "Wavelength conversion technologies for WDM network applications," J. Lightwave Technol. **14**(6), 955–966 (1996).
2. C. Langrock, S. Kumar, J. E. McGeehan, A. E. Willner, and M. M. Fejer, "All-optical signal processing using $\chi^{(2)}$ nonlinearities in guided-wave devices," J. Lightwave Technol. **24**(7), 2579–2592 (2006).
3. K. Gallo, G. Assanto, and G. I. Stegeman, "Efficient wavelength shifting over the erbium amplifier bandwidth via cascaded second order processes in lithium niobate waveguides," Appl. Phys. Lett. **71**(8), 1020–1022 (1997).
4. B. Chen and C.-Q. Xu, "Analysis of novel cascaded $\chi^{(2)}$ (SFG+DFG) wavelength conversions in quasi-phase-matched waveguides," IEEE J. Quantum Electron. **40**(3), 256–261 (2004).
5. K. J. Lee, S. Liu, F. Parmigiani, M. Ibsen, P. Petropoulos, K. Gallo, and D. J. Richardson, "OTDM to WDM format conversion based on quadratic cascading in a periodically poled lithium niobate waveguide," Opt. Express **18**(10), 10282–10288 (2010).
6. J. E. McGeehan, M. Giltrelli, and A. E. Willner, "All-optical digital 3-input AND gate using sum- and difference-frequency generation in a PPLN waveguide," Electron. Lett. **43**(7), 409–410 (2007).
7. Y. Wang, C. Yu, L. Yan, A. E. Willner, R. Roussev, C. Langrock, M. M. Fejer, J. E. Sharping, and A. L. Gaeta, "44-ns continuously tunable dispersionless optical delay element using a PPLN waveguide with two-pump configuration, DCF, and a dispersion compensator," IEEE Photon. Technol. Lett. **19**(11), 861–863 (2007).
8. K. J. Lee, F. Parmigiani, S. Liu, J. Kakande, P. Petropoulos, K. Gallo, and D. Richardson, "Phase sensitive amplification based on quadratic cascading in a periodically poled lithium niobate waveguide," Opt. Express **17**(22), 20393–20400 (2009).
9. S. Liu, K. J. Lee, K. Gallo, P. Petropoulos, and D. J. Richardson, "Elimination of the chirp of optical pulses through cascaded nonlinearities in periodically poled lithium niobate waveguides," Opt. Lett. **35**(22), 3724–3726 (2010).

#141703 - $15.00 USD Received 25 Jan 2011; revised 8 Mar 2011; accepted 8 Mar 2011; published 15 Apr 2011

10. S. Liu, K. J. Lee, F. Parmigiani, K. Gallo, P. Petropoulos, and D. J. Richardson, "Retiming of short pulses using quadratic cascading in a periodically poled lithium niobate waveguide," IEEE Photon. Technol. Lett. **23**(2), 94–96 (2011).
11. H. Ishizuki, T. Suhara, M. Fujimura, and H. Nishihara, "Wavelength-conversion type picosecond optical switching using a waveguide QPM-SHG/DFG device," Opt. Quantum Electron. **33**(7/10), 953–961 (2001).
12. Y. Wang, J. Fonseca-Campos, C.-Q. Xu, S. Yang, E. A. Ponomarev, and X. Bao, "Picosecond-pulse wavelength conversion based on cascaded second-harmonic generation-difference frequency generation in a periodically poled lithium niobate waveguide," Appl. Opt. **45**(21), 5391–5403 (2006).
13. J. Wang, J. Sun, X. Zhang, and D. Huang, "All-optical tunable wavelength conversion with extinction ratio enhancement using periodically poled lithium niobate waveguides," J. Lightwave Technol. **26**(17), 3137–3148 (2008).
14. J. Sun, H. Li, Y. Cheng, and J. Li, "Tunable wavelength conversion of picosecond pulses based on cascaded sum and difference-frequency generation in quasi-phase-matched $LiNbO_3$ waveguides," Opt. Commun. **281**(23), 5874–5883 (2008).
15. J. Wang, J. Sun, C. Luo, and Q. Sun, "Flexible all-optical wavelength conversions of 1.57-ps pulses exploiting cascaded sum- and difference frequency generation (cSFG/DFG) in a PPLN waveguide," Appl. Phys. B **83**(4), 543–548 (2006).
16. H. Furukawa, A. Nirmalathas, N. Wada, S. Shinada, H. Tsuboya, and T. Miyazaki, "Tunable all-optical wavelength conversion of 160-Gb/s RZ optical signals by cascaded SFG-DFG generation in PPLN waveguide," IEEE Photon. Technol. Lett. **19**(6), 384–386 (2007).
17. R. W. Boyd, *Nonlinear Optics*, 2nd ed. (Academic Press, 2003), Chap. 2.
18. G. Imeshev, M. A. Arbore, M. M. Fejer, A. Galvanauskas, M. Fermann, and D. Harter, "Ultrashort-pulse second-harmonic generation with longitudinally nonuniform quasi-phase-matching gratings: pulse compression and shaping," J. Opt. Soc. Am. B **17**(2), 304–318 (2000).
19. R. Eckardt and J. Reintjes, "Phase matching limitations of high efficiency second harmonic generation," IEEE J. Quantum Electron. **20**(10), 1178–1187 (1984).

1. Introduction

Efficient all-optical wavelength conversion is likely to be a key functionality within future wavelength-division-multiplexed (WDM) networks [1]. Wavelength conversion techniques exploiting cascaded second-order nonlinear processes in periodically poled lithium niobate (PPLN) waveguides have attracted much interest in recent years due to a number of attractive features relative to competitor approaches [2,3]. These features include high nonlinear coefficients allowing for compact devices, an ultra-fast optical response, broad wavelength conversion bandwidths within the telecom-band, bit-rate and modulation format transparency, and no excess noise accumulation. Two kinds of quadratic cascaded processes – namely cSHG/DFG and cSFG/DFG – have been employed for all-optical signal-processing with applications demonstrated including wavelength conversion [3,4], format conversion [5], logic gates [6], tunable optical time delays [7], phase sensitive amplification [8], chirp elimination [9], and pulse retiming [10].

In the various reports of wavelength conversion schemes based on either cSHG/DFG or cSFG/DFG, continuous wave (CW) and pulsed light have both been employed as either pump or signal waves for nonlinear cascading in the PPLN waveguide [11–16]. In order to apply these cascaded processes to practical digital communication systems, the transmitted signals should have the form of pulsed waves rather than CW signals – making a proper investigation of the wavelength conversion properties in the pulsed-pump regime especially important. There have been several theoretical and experimental studies of the cascaded processes in the CW-pump regime and the results show that the acceptable pump bandwidth for the SHG based approach is relatively narrow compared to the SFG case due to restrictions imposed by the quasi-phase matching (QPM) requirements [4]. However, no consistent study has been performed to compare the cSHG/DFG and cSFG/DFG schemes in the pulsed-pump regime, in which the acceptance bandwidth should have a somewhat different definition since it actually depends on the input pump conditions.

In this paper, we report the first systematic study on the acceptance bandwidths under pulsed pump operation of the cSHG/DFG and the cSFG/DFG processes. The acceptance bandwidths of SHG and SFG are first carefully compared in the CW and the pulsed-pump regimes via both modelling and experiments. The results show that these bandwidths are comparable in the pulsed-pump regime, while the SHG bandwidth is half that of SFG in the CW-pump regime. As a consequence we conclude that the tuning bandwidths of both

#141703 - $15.00 USD Received 25 Jan 2011; revised 8 Mar 2011; accepted 8 Mar 2011; published 15 Apr 2011

cascaded processes should be similar in the pulsed pump regime (i.e. the cSHG/DFG bandwidth is not limited by the CW SHG bandwidth). We go on to confirm that this is the case experimentally.

2. Theoretical analysis

2.1 CW-pumped SHG and SFG

The schematic diagrams of the CW-pumped SHG and SFG processes in a PPLN waveguide are illustrated in Figs. 1(a) and 1(b), respectively. The second harmonic (SH) wave of an input pump (CW_0) is generated by the SHG process, whereas the sum-frequency (SF) wave is generated from two pump beams (CW_1 and CW_2) by the SFG process as shown in Figs. 1(a) and 1(b). In order to investigate the acceptance bandwidths for each case, the pump wavelengths of CW_0 in Fig. 1(a) and CW_2 in Fig. 1(b) are tuned around the resonant wavelengths that satisfy the QPM condition. Then the phase mismatch for SHG around the resonant pump frequency (ω_0) is defined by [17],

$$\Delta k_{SHG}(\Delta\omega) = 2k(\omega) - k(2\omega) \equiv 2k(\omega_0 + \Delta\omega) - k(2\omega_0 + 2\Delta\omega), \tag{1}$$

which can be rewritten using a Taylor expansion as follows:

$$\begin{aligned} \Delta k_{SHG}(\Delta\omega) &= 2k(\omega_0) - k(2\omega_0) + 2\left[\left.\frac{\partial k}{\partial\omega}\right|_{\omega_0} - \left.\frac{\partial k}{\partial\omega}\right|_{2\omega_0}\right]\Delta\omega + O(\Delta\omega^2) \\ &= \Delta k_{0,SHG} + 2\left[\frac{1}{u_0} - \frac{1}{u_{SH}}\right]\Delta\omega + O(\Delta\omega^2). \end{aligned} \tag{2}$$

Here, $\Delta k_{0,SHG}$, u_0, and u_{SH} denote the phase mismatch at ω_0 and the group-velocities of the pump (CW_0) and SH waves, respectively. The function O denotes the rest of the series beyond the second order. In the same way, the phase mismatch for SFG can be derived as,

$$\Delta k_{SFG}(\Delta\omega) = \Delta k_{0,SFG} + \left[\frac{1}{u_2} - \frac{1}{u_{SF}}\right]\Delta\omega + O(\Delta\omega^2), \tag{3}$$

where, $\Delta k_{0,SFG}$, u_2, and u_{SF} also denote the phase mismatch at resonance and the group-velocities of the tunable pump (CW_2) and SF waves, respectively.

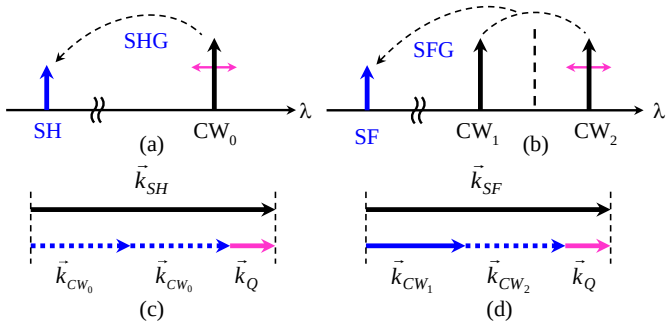

Fig. 1. Schematic diagrams of (a) SHG and (b) SFG processes in the CW-pump regime. The wave vector mismatches for (c) SHG and (d) SFG. The solid and dashed lines representing each vector correspond to the fixed and the tunable wavelength, respectively.

If the pumps in both the SHG and SFG cases are in the same frequency band, i.e. $\omega_0 \approx \omega_2$ (and as a consequence, $\omega_{SH} \approx \omega_{SF}$), the group velocity mismatches (GVMs) in each case can be considered to take approximately the same value, as follows:

#141703 - $15.00 USD Received 25 Jan 2011; revised 8 Mar 2011; accepted 8 Mar 2011; published 15 Apr 2011

$$\frac{1}{u_0} - \frac{1}{u_{SH}} \cong \frac{1}{u_2} - \frac{1}{u_{SF}} \cong \delta\nu. \tag{4}$$

In the experiments described in section 3, their difference is only 0.05%, and thus is negligible in our analysis. Since both $\Delta k_{0,SHG}$ and $\Delta k_{0,SFG}$ in Eqs. (2) and (3) are equal to zero at the QPM resonance, the phase mismatches in each case [Eqs. (2) and (3)] can be rewritten as,

$$\Delta k_{SHG} \cong 2\delta\nu \cdot \Delta\omega, \tag{5}$$

$$\Delta k_{SFG} \cong \delta\nu \cdot \Delta\omega, \tag{6}$$

which indicates that the phase mismatch for SHG varies almost twice as rapidly as for the SFG counterpart. The output powers of SH and SF in Ref. [17]. can then be expressed as,

$$P_{SH} \propto \mathrm{sinc}^2\left(\frac{\Delta k_{SHG} L}{2}\right) \cong \mathrm{sinc}^2\left(\delta\nu \cdot \Delta\omega\right), \tag{7}$$

$$P_{SF} \propto \mathrm{sinc}^2\left(\frac{\Delta k_{SFG} L}{2}\right) \cong \mathrm{sinc}^2\left(\frac{\delta\nu \cdot \Delta\omega}{2}\right), \tag{8}$$

showing that the CW acceptance bandwidth for SFG is twice as broad as for the SHG counterpart.

The broader pump bandwidth in the SFG case can also be explained in Figs. 1(c) and 1(d) illustrating the wave-vector mismatches for each case. Here, each *k* vector denotes the wave-vectors of the SH, CW_0, CW_1, and CW_2, respectively. The QPM grating vector, k_Q, is defined by $2\pi/\Lambda$, where Λ denotes the QPM grating period. The solid and dashed lines of each vector also represent the fixed and the tunable wavelength, respectively. In the SFG case [Fig. 1(d)], CW_2 is tunable while the wavelength of CW_1 is fixed as defined in Fig. 1(b). Therefore, the wavelength tuning of CW_2 affects only the wave vector of CW_2. In the SHG case, however, the tuning of the pump wave (CW_0) simultaneously changes two degenerate pump vectors as shown in Fig. 1(c), which means the QPM condition is more readily broken under wavelength tuning as compared to the SFG case. Therefore, the SH power is more sensitive to variation of the pump wavelength, resulting in a narrower acceptance bandwidth as compared to the SFG case.

2.2 Pulsed-pump SHG and SFG

Now the pulsed-pumped SHG and SFG processes in a PPLN waveguide are investigated. The schematic diagrams for each case are illustrated in Figs. 2(a) and 2(b), respectively. The configuration of the interacting waves is very similar to that of Fig. 1, other than two pulsed-pumps (Pulse 0, 2) are used as tunable sources instead of the CW pumps.

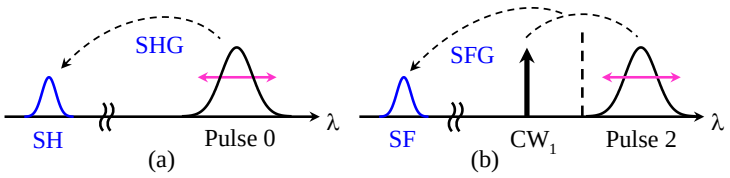

Fig. 2. Schematic diagrams of (a) SHG and (b) SFG processes in the pulsed-pump regime.

In order to deal with the short-pulse nonlinear frequency conversion schemes, we consider the simpler frequency domain picture rather than the time domain model. The converted output fields can be expressed as the product of the Fourier transforms of the input pump fields and the spectral filter function (*D*) associated to the QPM grating in the PPLN waveguide [18]. In our cases, the output SH and the SF fields can be expressed as follows:

#141703 - $15.00 USD Received 25 Jan 2011; revised 8 Mar 2011; accepted 8 Mar 2011; published 15 Apr 2011

$$\tilde{A}_{SH}(\Omega) = D_{SHG}(\Omega)\cdot[\tilde{A}_0^2(\Omega)], \tag{9}$$

$$\tilde{A}_{SF}(\Omega) = D_{SFG}(\Omega)\cdot[\tilde{A}_1(\Omega) * \tilde{A}_2(\Omega)], \tag{10}$$

where, Ω and each $\tilde{A}_i(\Omega)$ denote the frequency offset and the Fourier transforms of the interacting waves, respectively. The asterisk in Eq. (10) denotes the convolution integral between two interacting pump fields (CW_1 and Pulse 2). In the SFG case of Fig. 2(b), the optical fields of the CW- and the pulsed-pumps in the frequency domain are expressed as:

$$A_1(t) \equiv \text{CW} \rightarrow \tilde{A}_1(\omega) = \delta(\omega - \omega_1), \tag{11}$$

$$A_2(t) \equiv \text{Pulsed} \rightarrow \tilde{A}_2(\omega), \tag{12}$$

and therefore, Eq. (10) can be rewritten as follows:

$$\tilde{A}_{SF}(\Omega) = D_{SFG}(\Omega)\cdot[\tilde{A}_2(\Omega)]. \tag{13}$$

In order to correctly investigate the acceptance bandwidths for the SHG and the SFG in the pulsed-pump regime, the spectral widths of input fields [$A_0(\Omega)$ and $A_2(\Omega)$] in Eqs. (9) and (13) are assumed to be broader than the bandwidths of their filter functions. In this instance then the filter functions primarily determine the widths of both the SH and the SF fields. These filter functions depend on the following phase mismatches for each process. The latter are originally to be derived as a function of two variables (frequency offsets) as in Ref. [18], yet to first-order they reduce to a function of only one of them (namely the pump frequency offset from resonance hereafter denoted by Ω) and can be expressed as follows:

$$\Delta k_{SHG}(\Omega) = \Delta k_{0,SHG} + \left[\frac{1}{u_0} - \frac{1}{u_{SH}}\right]\Omega + O(\Omega^2), \tag{14}$$

$$\Delta k_{SFG}(\Omega) = \Delta k_{0,SFG} + \left[\frac{1}{u_2} - \frac{1}{u_{SF}}\right]\Omega + O(\Omega^2). \tag{15}$$

Here, u_0, u_2, u_{SH}, and u_{SF} denote the group-velocities of Pulse 0, Pulse 2, SH and SF waves, respectively. In the same pump frequency band, the GVM values can be assumed to have the same value again as given in Eq. (4), and then we can get the phase mismatches in Eqs. (14) and (15) as follows:

$$\Delta k_{SHG}(\Omega) \cong \delta\nu\cdot\Omega, \tag{16}$$

$$\Delta k_{SFG}(\Omega) \cong \delta\nu\cdot\Omega. \tag{17}$$

It should be noted that the factor of 2 in the CW-pump case [Eq. (5)] has disappeared in the pulsed-pump case [Eq. (16)] and that the two phase mismatches vary in the same way with Ω. Now the filter functions can be expressed as follows:

$$D_{SHG}(\Omega) \propto \int_0^L e^{-i\Delta k_{SHG}(\Omega)z}dz = \int_0^L e^{-i\delta\nu\cdot\Omega z}dz, \tag{18}$$

$$D_{SFG}(\Omega) \propto \int_0^L e^{-i\Delta k_{SFG}(\Omega)z}dz = \int_0^L e^{-i\delta\nu\cdot\Omega z}dz = D_{SHG}(\Omega), \tag{19}$$

which means that both the SHG and the SFG cases have essentially the same filter function. Although the SH and the SF output fields are determined by Eqs. (9) and (13), the relatively narrower filter functions select only a certain part of the spectral components from their input pump fields, which leads to similar widths for both the SH and the SF output fields.

#141703 - $15.00 USD Received 25 Jan 2011; revised 8 Mar 2011; accepted 8 Mar 2011; published 15 Apr 2011

Therefore, the acceptance pump bandwidths for the SHG and the SFG processes are comparable with each other in the pulsed-pump regime.

This observation can be intuitively explained by the following physical considerations. In the case of Fig. 2(a), the symmetric spectral components on both sides of the resonant wavelength for the SHG also interact with each other as two pulsed pumps for SFG. Therefore, the energy of the input pulse that falls outside of the SHG filter bandwidth is not wasted but used to generate SF pulses at the same wavelength as the SH. This intuitive picture is also linked in our theoretical description in Eq. (9).

3. Experiment and discussion

Figure 3(a) shows the experimental setup we used to measure the acceptance bandwidths for the SHG and the SFG in the CW-pump regime. A 30-mm-long fibre pigtailed PPLN waveguide (HC Photonics Corp.) was used for both the SHG and the SFG processes, and its SHG phase matching wavelength was 1546 nm at 50°C. In the SHG case, only the tunable source CW_1 was launched into the waveguide (which was labelled as CW_0 in Fig. 1(a)), while both the CW_1 with a fixed wavelength and the tunable CW_2 were used as two pump sources for the SFG case. Figures 3(b) and 3(c) show the normalised powers of the SH and the SF waves plotted as a function of the pump wavelength, respectively. The bandwidths measured in each case were 0.38 nm for SHG and 0.73 nm for SFG respectively. As discussed in the previous section, the SHG bandwidth was narrower than its SFG counterpart, which confirms the ideas mentioned above and in Ref. [4]. The SHG bandwidth was not exactly half of the SFG counterpart due to the small difference between the pump wavelengths in each case. As can be seen in Figs. 3(b) and 3(c), they are well matched with the points in the theoretical curves calculated using Eqs. (7) and (8).

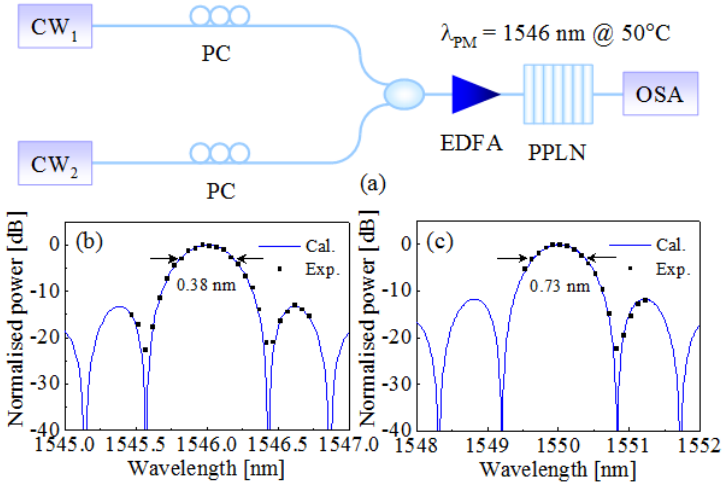

Fig. 3. (a) Experimental setup used for the measurement. Both CW_1 and CW_2 are used for the case of Fig. 1(b), while only CW_1 (which is labelled as CW_0 in Fig. 1(a)) is used for the case of Fig. 1(a). PC: polarisation controller, EDFA: erbium-doped fibre amplifier, OSA: optical spectrum analyser. The measured and calculated bandwidths for (b) the SHG and (c) the SFG.

Next the pulsed-pump quadratic cascaded processes were investigated. The schematic diagrams of the cSHG/DFG and the cSFG/DFG in a PPLN waveguide are shown in Figs. 4(a) and 4(b), respectively. In the case of cSHG/DFG, a short pulse with a spectral width broader than the CW acceptable bandwidth for the SHG is used as the pump beam. The generated SH pulse then interacts with the CW signal ($CW_{1,\,SIG}$) by the DFG, resulting in the output pulse as shown in Fig. 4(a). In the cSFG/DFG process, a CW_1 and a pulsed signal interact with each other as the two pump sources for the SFG. Then the generated SF wave interacts with CW_2 through DFG to produce the output pulsed signal as shown in Fig. 4(b). The experimental setups used to measure the acceptance bandwidths for each case are illustrated in Fig. 4(c). An

#141703 - $15.00 USD Received 25 Jan 2011; revised 8 Mar 2011; accepted 8 Mar 2011; published 15 Apr 2011

erbium glass oscillator (ERGO) was used as the pulsed pump source. It generated 10 GHz, 2-ps pulses with a corresponding spectral bandwidth of ~2.1 nm. The central wavelengths of the ERGO were 1546 nm for the cSHG/DFG [Fig. 4(a)] and 1550 nm for the cSFG/DFG [Fig. 4(b)], respectively. There was the option to filter the pump pulses using a 1.0 nm-bandpass filter which restricted their temporal width to 4 ps. The pulses were then modulated by a 2^{31} – 1 pseudorandom bit sequence (PRBS) using a lithium niobate modulator. In the case of Fig. 4(a), only CW_1 (1538 nm) was used as the CW signal (which is labelled as $CW_{1,\,SIG}$ in Fig. 4(a)), while both CW_1 (1542 nm) and CW_2 (1558 nm) were used as pump and signal beams for the case of Fig. 4(b), respectively. The inputs were then combined in a 3-dB coupler and launched into the PPLN waveguide after amplification.

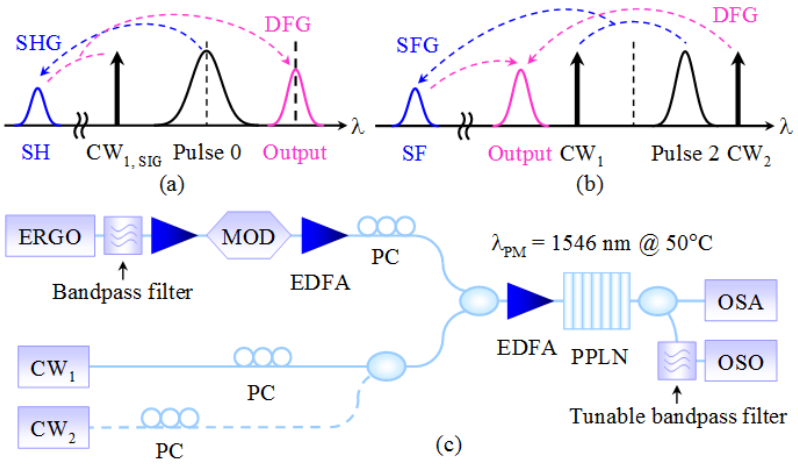

Fig. 4. Schematic diagrams of (a) the cSHG/DFG and (b) the cSFG/DFG processes in the pulsed pump-regime. (c) Experimental setup used to measure the acceptable bandwidths for each case. Only CW_1 is used for the case of (a), while both CW_1 and CW_2 are used for the case of (b). ERGO: Erbium doped glass oscillator, MOD: modulator, OSO: optical sampling oscilloscope.

The spectral and temporal shapes for each case, as monitored with an optical spectrum analyser (OSA) and an optical sampling oscilloscope (OSO), are presented in Fig. 5 and Fig. 6, respectively. The measured optical signal-to-nose ratios (OSNR) of the converted output waves were 16 dB at 1554.1 nm for the cSHG/DFG [Fig. 4(a)] and 15.7 dB at 1534.2 nm for the cSFG/DFG [Fig. 4(b)], respectively. The temporal shapes of the output pulses measured without the 1.0-nm filter were distorted as shown in Fig. 5(d) and Fig. 6(d), which is due to the distortion of the SH (or SF) waves caused by the group delay between the SH (or the SF) and the pump waves in the PPLN waveguide [12].

Now we compare the results measured with the 1.0-nm filter. In the case of cSHG/DFG, if the acceptance bandwidth for the SHG were approximately half of the SFG bandwidth as in the case of the CW-pump regime, then one would expect the temporal width of the output pulse [Fig. 5(b)] to be much broader than the pulse width in the cSFG/DFG case [Fig. 6(b)]. However, as indicated in Figs. 5(b) and 6(b), the temporal width of the cSHG/DFG output was comparable with its cSFG/DFG counterpart in the pulsed-pump regime, and the measured spectral bandwidths of each case were 1.1 nm for the cSHG/DFG [Fig. 5(a)] and 1.0 nm for the cSFG/DFG [Fig. 6(a)], respectively. As discussed in section 2.2, this is because the filter functions for the SHG and SFG processes are essentially the same in the pulsed-pump regime, which leads to the comparable output pulse widths in the two cascaded processes. The small difference between the measured spectral (and temporal) widths in each case was due to the slightly different spectral positions of the interacting wavelengths for each cascaded process.

#141703 - $15.00 USD Received 25 Jan 2011; revised 8 Mar 2011; accepted 8 Mar 2011; published 15 Apr 2011

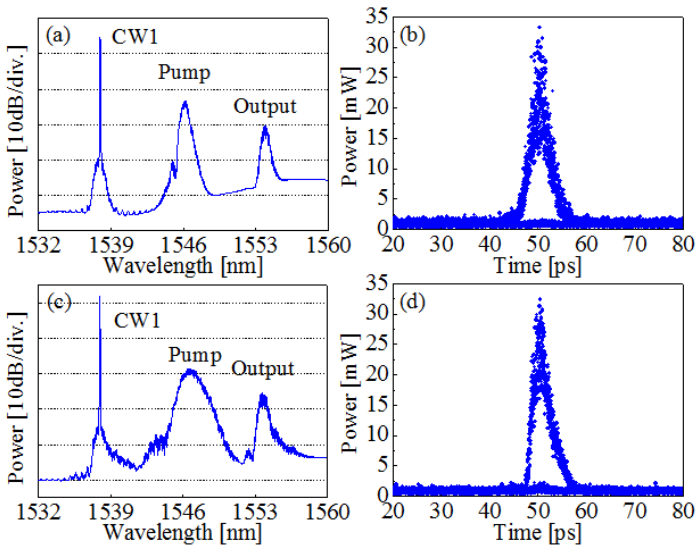

Fig. 5. Measured spectral and temporal shapes for (a) 1.0 nm filters and (b) without the filter in the cSHG/DFG.

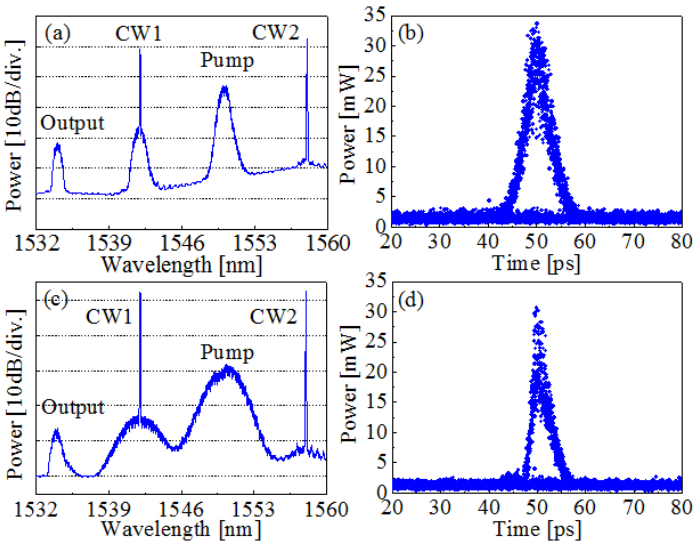

Fig. 6. Measured spectral and temporal shapes for (a) 1.0 nm filters and (b) without the filter in the cSFG/DFG.

4. Conclusion

When the pump signals involved in quadratic processes in a quasi-phase-matched waveguide, such as a PPLN device, are CW waves, the acceptance bandwidth for SFG is almost twice as broad as compared to the corresponding bandwidth of the SHG process. This is because phase matching of the two degenerate pump vectors involved in SHG is more sensitive to small detunings from the nominal wavelength than in the corresponding case of SFG. We have shown in this paper that this relation is no longer valid when spectrally broader pumps are considered, i.e. when the pumps are pulsed. In this case, the spectral wings of the pulses interact with each other in a similar fashion as the different pump signals in SFG, resulting in an effectively broader acceptance bandwidth than in the CW-case. We have demonstrated this

#141703 - $15.00 USD Received 25 Jan 2011; revised 8 Mar 2011; accepted 8 Mar 2011; published 15 Apr 2011

effect both analytically as well as experimentally, where nonlinear conversion experiments based on either cSHG/DFG or cSFG/DFG with a broadband pump have confirmed that the width of the converted signal was similar in both cases, even if the pump bandwidth exceeded the nominal (CW-based) acceptance bandwidth of the SHG process. Our analysis neglected nonlinearly-induced phase-mismatches which can in principle be expected in strong pump depletion regimes for e.g. SHG [19], as well as third-order effects, for which we found no evidence in our experimental conditions. We expect that our results will be useful for applying the two quadratic cascaded processes to short-pulse wavelength converters in practical digital communication systems.

Acknowledgment

This work was supported by the UK Engineering and Physical Sciences Research Council (EPSRC) under grant agreement EP/F032218/1. Katia Gallo gratefully acknowledges support from the European Union (EU) under grant agreement PIEF-GA-2009-234798.

#141703 - $15.00 USD Received 25 Jan 2011; revised 8 Mar 2011; accepted 8 Mar 2011; published 15 Apr 2011